Photonic sintering via flash white light combined with deep UV and NIR for $SrTiO_3$ thin film vibration touch panel applications

2016 Nanotechnology 27 505209

(http://iopscience.iop.org/0957-4484/27/50/505209)

IOP Publishing Nanotechnology
Nanotechnology 27 (2016) 505209 (6pp) doi:10.1088/0957-4484/27/50/505209

Photonic sintering via flash white light combined with deep UV and NIR for $SrTiO_3$ thin film vibration touch panel applications

Hyun-Jun Hwang[1,5], Soo-Chul Lim[2,5], Kyung-Chul Ok[3], Jin-Seong Park[3] and Hak-Sung Kim[1,4]

[1] Department of Mechanical Engineering, Hanyang University, Haengdang-dong, Seongdong-gu, Seoul 133-791, Korea
[2] Department of Mechanical, Robotics and Energy Engineering, Dongguk University-Seoul, Seoul 100-715, Korea
[3] Division of Materials Science and Engineering, Hanyang University, Haengdang-dong, Seongdong-gu, Seoul 133-791, Korea
[4] Institute of Nano Science and Technology, Hanyang University, Seoul, 133-791, Korea

E-mail: kima@hanyang.ac.kr

Received 2 September 2016, revised 27 October 2016
Accepted for publication 3 November 2016
Published 18 November 2016

Abstract

An ultra-high speed photonic sintering method consisting of flash white light (FWL) combined with near infrared (NIR) and deep UV light irradiations was developed to fabricate a $SrTiO_3$ (STO) thin film for application in electro-vibration touch panels. The STO thin film was sintered on PEN by FWL irradiation at room temperature under ambient conditions, which is a dramatically simple and ultrahigh speed fabrication process compared to the conventional high temperature (600 °C–900 °C) thermal sintering process. The effects of the FWL irradiation conditions (energy density, pulse numbers, and pulse duration) on the dielectric constant of the sintered STO thin films were evaluated. Furthermore, the effects of NIR and deep UV irradiation during the FWL sintering process were also investigated.

Keywords: vibration touch panel, $SrTiO_3$, flash white light, near infrared, deep ultraviolet

(Some figures may appear in colour only in the online journal)

1. Introduction

Interest in designing and investigating haptic interfaces for touch-based interactive systems has been growing rapidly [1–6]. Due to the popularity of touch-based interfaces both in research and end-user communities, interest in these interfaces has accelerated rapidly. Recently, an alternative haptic interface using the principle of electro-vibration without any mechanical actuator was developed and applied to various applications due to its several compelling properties [7–9]. For example, it is fast, low-powered, dynamic, and can be used in a wide range of interaction scenarios and applications, including multi-touch interfaces as well as flexible, curved, and irregular touch surfaces. The tactile feedback based on electro-vibration is driven by electrostatic friction between the touch screen surface and the user's fingers [10, 11]. The feeling of friction only appears when there is an insulating barrier between the conductive surface and the sliding finger. Thus, a thin dielectric layer should be coated on a conductive electrode in electrovibration-based tactile displays [7]. Conventionally, dielectric materials such as HfO and SiO_2 have been applied to the dielectric layer, because of their excellent permittivity and stability. However, these materials need a high voltage for modulating the perceived friction. When a high electric potential is applied to a thin layer of the dielectric materials, the current leakage occurs easily causing the decrease of the efficiency of the device [12–14]. For these reasons, a high-K material has been required to modulate the perceived friction even at a low voltage for the commercialization.

[5] These authors contributed equally to this work.

In these circumstances, thin films made of high dielectric constant materials based on the alkaline earth titanate of $SrTiO_3$ (STO) have received much attention due to their large electro-optical coefficient, low optical losses, and excellent optical transparency in the visible region [15, 16]. Conventionally, STO thin films are sintered by high temperature (~900 °C) thermal sintering [17, 18]. However, high temperature processes can cause fatal problems, causing damage to flexible polymer substrates such as polyethylene terephthalate (PET) and polyethylene naphthalate (PEN). Moreover, the thermal sintering method has limitations for mass production because of its low throughput and environmental obstacles, such as the requirement of a chamber.

To overcome these limitations, in this work, a new way to fabricate STO thin films by using a photonic sintering method was demonstrated. Flash white light (FWL) irradiation can instantly sinter strontium titanate ($SrTiO_3$) thin films on ITO-coated PEN at room temperature under ambient conditions in a few milliseconds without damaging the substrate, which is a dramatically simple, ultra-high speed, and one-shot large area fabrication process compared to the conventional high temperature thermal sintering process [19, 20]. Meanwhile, we wondered what would happen when light with a wavelength longer or shorter than FWL (visible light) is applied, because the behavior of electromagnetic radiation depends on its wavelength. For this reason, the NIR- or deep UV-assisted FWL sintering method was suggested and demonstrated by irradiating the films with NIR and deep UV during the FWL sintering process of STO thin films (figure 1). The effects of the FWL irradiation conditions (energy density, pulse number, and pulse duration) and the power of the NIR/deep UV on the dielectric constant of STO thin films were evaluated using several microscopic and spectroscopic characterization techniques, including SEM and XRD.

2. Materials and methods

2.1. Material preparation and fabrication of $SrTiO_3$ thin films

For the fabrication of $SrTiO_3$ (STO) thin films for electro-vibration touch panels, strontium titanate (ST) solutions with a concentration of 0.75 M were prepared by dissolving strontium acetate ($(CH_3CO_2)_2Sr$, 99.995%; Sigma Aldrich) in heated acetic acid. Titanium IV isopropoxide (99.999%; Sigma Aldrich) was then added, followed by the addition of ethylene glycol (99.5%; Samchun) in an acetic acid:ethylene glycol solution ($R_{ac/e.g.}$ ratio of 1:1). Finally, the solution was heated to promote the condensation reaction between acetic acid and ethylene glycol [21]. All of the materials mentioned above were thoroughly mixed to prepare a stable solution with a uniform composition [22, 23]. A spin-coating technique was employed to deposit the mixed solution onto ITO PEN substrates.

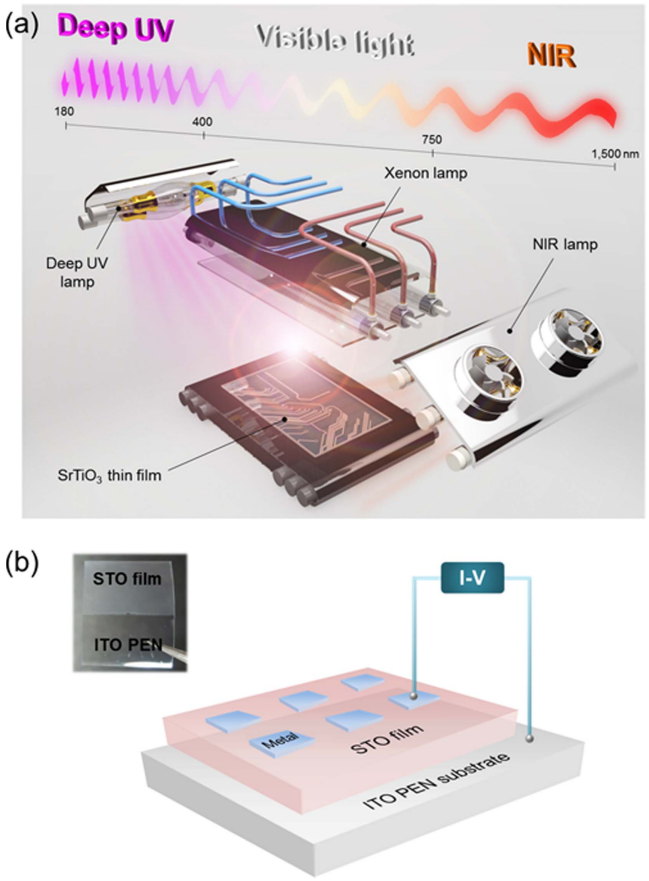

Figure 1. Schematics of the photonic sintering of STO thin films using flash white light (FWL), NIR, and deep UV (a); and the measurement of dielectric constant of STO thin film coated on ITO PEN substrate (b).

2.2. Photonic sintering method

The deposited STO films were sintered by FWL combined with NIR and deep UV irradiation at room temperature under ambient conditions (figure 1). White light from a xenon flash lamp has a broad wavelength range from 380 nm to 950 nm. In addition, a commercial deep UV system (100 mW, LUMATEC SUV-DC) with a wavelength range from 180 nm to 280 nm and an NIR system (500 W, Adphos L40) with a wavelength range of 800–1500 nm were used in this study (see inset in figure 1(a)). To optimize the photonic sintering conditions, the irradiation energy of FWL, the power of deep UV, and the irradiation time of NIR were varied.

2.3. Characterization

The microstructures, surface, and thickness of the sintered STO films were examined via scanning electron microscopy (SEM, S4800 Hitachi). To confirm the STO films structure on the conductive substrate (ITO PEN) after NIR- or deep UV-assisted FWL irradiation, crystal phase analysis was performed using x-ray diffraction (XRD, D/MAX RINT 2000, CuKα radiation). The dielectric constant of STO films were measured at 10 kHz, using a semiconductor parameter analyzer module (Agilent 4284A and 4155A).

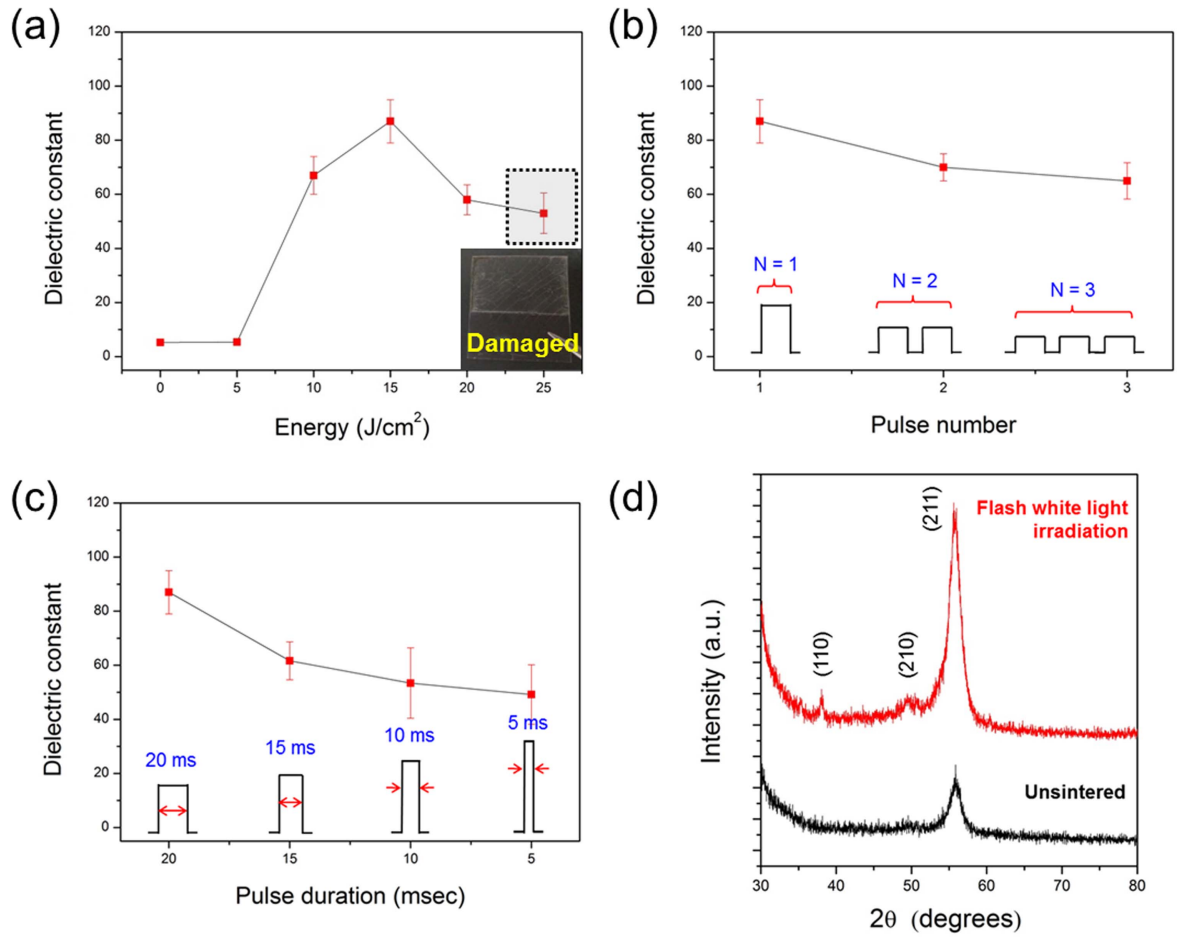

Figure 2. Flash white light (FWL) sintering of STO films. The dielectric constants of the FWL sintered STO films with variation of the energy density (a), pulse number (b), and pulse duration (c). XRD patterns of STO films before- and after FWL irradiation (d).

3. Results and discussion

To sinter the STO films, we used FWL with an energy density ranging from 5–25 J cm^{-2} where a single pulse with a duration of 20 ms was applied. As shown in figure 2(a), the dielectric constant of the STO films began to be measured when the irradiation energy was higher than 10 J cm^{-2}. An irradiation energy less than 5 J cm^{-2} was insufficient to sinter the STO thin films. Meanwhile, it was also found that the dielectric constant increased as the irradiation energy increased up to 15 J cm^{-2}. In the unsintered STO film, STO nanoparticles were surrounded by a residual binder, which resulted in a blurry SEM image (figure 3(a)). With an FWL irradiation of 15 J cm^{-2}, the binder was evaporated, allowing STO nanoparticles to be observed more clearly (figure 3(b)). Then, the STO nanoparticles were sintered, resulting in an increase of the dielectric constant. However, the dielectric constant decreased again when the FWL was higher than 20 J cm^{-2} because the STO films were damaged due to excessive irradiation energy, as shown in the inset in figure 2(a).

To investigate the effect of the number of pulses, the number was varied while the total energy was maintained at 15 J cm^{-2}. Figure 2(b) shows that the dielectric constant of the STO films decreased as the number of pulses increased. The single pulse produced better dielectric characteristics than multiple pulses since the intensity of the pulse decreased as the pulse number increased in order to maintain the same total energy. For these reasons, the STO films were not sintered fully when irradiated by multiple pulses.

In addition, with a total irradiation energy of 15 J cm^{-2}, the duration of the single pulse was varied to investigate the effect of the pulse duration. As shown in figure 2(c), the dielectric constant of the STO films decreased with decreasing pulse duration. When the total energy was maintained, a shorter pulse duration results in an increase of the pulse intensity, as shown in inset in figure 2(c). For this reason, when irradiated by FWL pulses shorter than 15 ms, STO films were damaged due to the high intensity of the pulses. Therefore, it was concluded that an irradiation energy of 15 J cm^{-2} with a single pulse duration of 20 ms were the optimal conditions for sintering the STO films.

Figure 2(d) shows the XRD patterns of the unsintered and FWL sintered-STO films. It was observed that the STO (211) peak increased and the peaks of (110) and (210) emerged after FWL irradiation. This indicates that the STO films became a polycrystalline microstructure with (110), (210), and (211) orientations and were sintered by FWL irradiation. These results correspond to those obtained from the SEM analysis (figure 3(b)). Therefore, it was

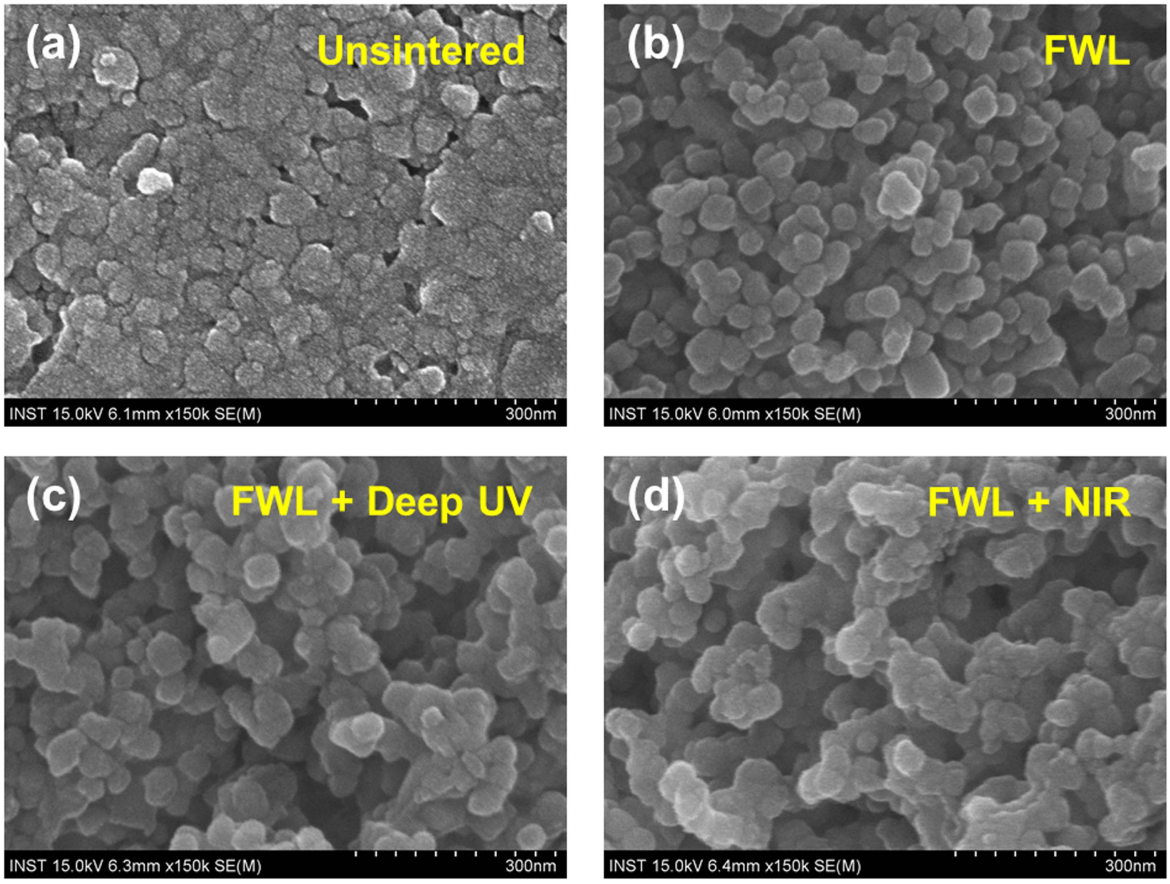

Figure 3. The SEM images of STO films before- and after- photonic sintering process using FWL (energy density: 15 J cm^{-2}, pulse duration: 20 ms, pulse number: 1), deep UV (irradiation power: 30 mW cm^{-2}), and NIR (irradiation power: 3 W cm^{-2}, irradiation time: 180 s).

demonstrated that STO films can be sintered by FWL irradiation under ambient conditions.

Deep UV was also used together during the FWL sintering of STO films where the power of deep UV was varied from 30 to 90 mW cm^{-2}, whereas the FWL was irradiated with an energy density of 15 J cm^{-2} with a single pulse and 10 ms duration. As shown in figure 4(a), it was found that deep UV with an irradiation of 30 mW cm^{-2} during the FWL sintering process resulted in a considerable increase of the dielectric constant of the STO films. It was also observed that deep UV-assisted FWL sintering led to an increase of the grain size of STO nanoparticles compared to those sintered by FWL only, as shown in the SEM images (figures 3(b) and (c)). This is because the STO films absorbed photonic energy effectively due to their photo-catalytic phenomena [24]. The photo-catalytic activity of STO occurs only when photons with energies greater than the band-gap energy of STO result in the excitation of electrons, which can promote reaction [25]. Deep UV with a wavelength of 280 nm has an energy of 4.43 eV, which is greater than the bandgap energy of STO (3.75 eV), so that can be absorbed in STO films and provide films with a sufficient energy. For these reasons, the irradiation of deep UV with high energies enhanced the sintering of STO through the photo-catalytic reaction. As shown in the XRD pattern (see the blue line in figure 4(c)), it was demonstrated that the crystallization of STO proceeded in the (111), (200), and (210) directions, resulting in an increase of the dielectric property. However, the dielectric constant decreased again when deep UV was irradiated with a power higher than 60 mW cm^{-2} (figure 4(a)). This may be because the excessive energy of deep UV caused damage of the STO films.

To further enhance the efficiency of the photonic sintering of STO thin films, NIR irradiation was also applied with FWL sintering (figure 4(b)). NIR with a power of 3 W cm^{-2} was radiated onto the STO films for 0–180 s, followed by FWL irradiation. It is noteworthy that the dielectric constant of the STO films increased as the irradiation time of NIR was longer over the entire energy conditions of the FWL. This is because the longer irradiation time of NIR induced a higher temperature of the STO films [26]. Temperature is one of the dominant thermodynamic variables for sintering. Sintering at a higher temperature enhances the densification rate relative to the grain growth rate [27]. For these reasons, additional NIR irradiation before FWL sintering could enhance the perovskite phase of STO films through the photo-thermal reaction. When the FWL energy was 15 J cm^{-2} with NIR treatment for 180 s, the highest dielectric constant was obtained, which was even higher than the case of deep UV-assisted FWL sintering (figure 4(d)). However, when the energy of FWL was higher than 20 J cm^{-2}, the dielectric constant decreased again, consistent with the case of FWL

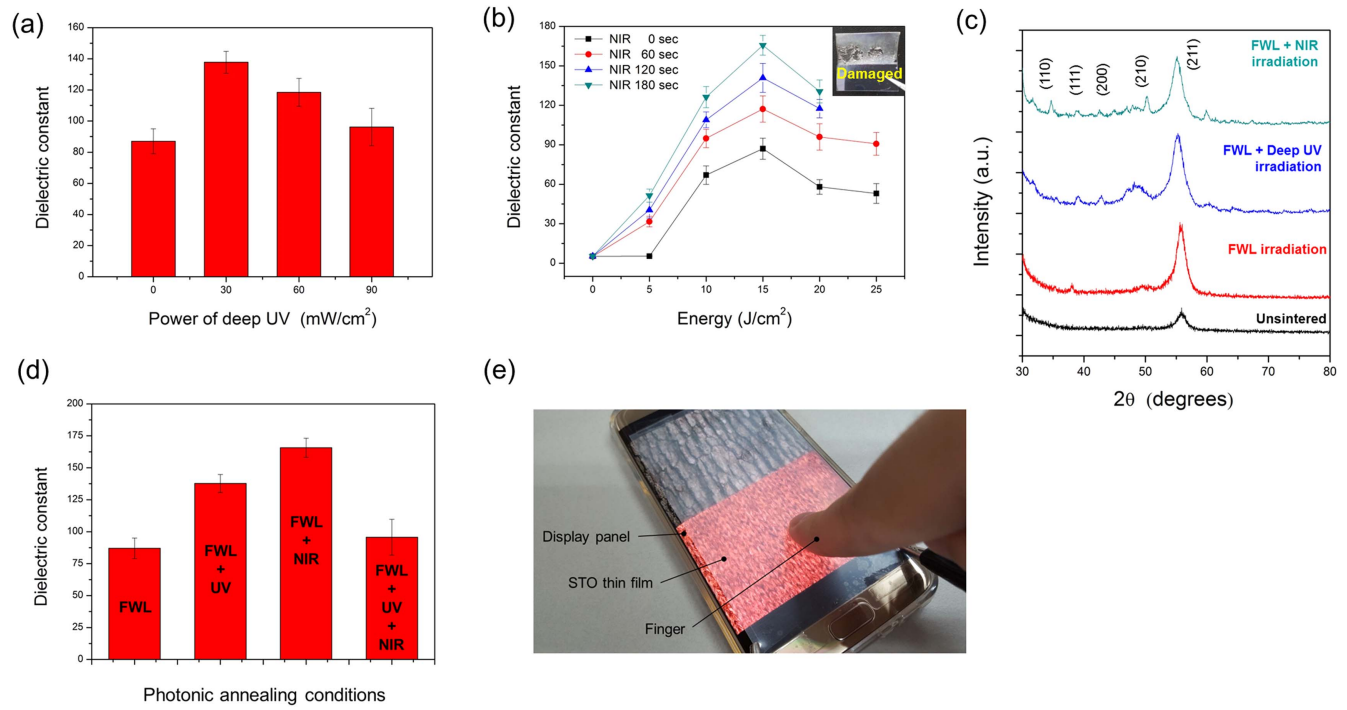

Figure 4. Deep UV/NIR-assisted flash white light (FWL) sintering of STO films. (a) The dielectric constants of STO films sintered by FWL combined with deep UV irradiation. (b) The dielectric constants of STO films sintered by FWL with NIR pre-treatment. (c) XRD patterns of the STO films sintered by FWL, deep UV, and NIR. (d) Comparison of the dielectric constant of STO films sintered by light irradiations with various wavelength conditions (FWL: 15 J cm^{-2} with single pulse of 20 ms, Deep UV: 30 mW cm^{-2}, and NIR: 3 W cm^{-2} for 180 s). (e) Application of the photonic sintered STO thin film to electro-vibration touch panel controlling electrostatic friction between a touch surface and the user's finger.

only (figure 4(b)). Moreover, with NIR irradiation longer than 120 s, a FWL of 25 J cm^{-2} caused damage of the STO films and PET substrate, as shown in the inset in figure 4(b), so that the dielectric constants could not be measured. Figure 3 shows that the STO nanoparticles irradiated by FWL combined with NIR were agglomerated more densely than those sintered by FWL only or deep UV-assisted FWL, resulting in an increase of the dielectric property. Furthermore, the XRD pattern of the STO film sintered by FWL combined with NIR irradiation (see the green line in figure 4(c)) shows that the peaks of STO were sharper than the other patterns, demonstrating that a high-quality STO polycrystalline film was obtained by FWL combined with NIR. These findings correspond to the results of the SEM images (figure 3). Therefore, it was demonstrated that highly dielectric STO films were successfully produced on the flexible PEN substrate by FWL irradiation (15 J cm^{-2} energy density, single pulse, and 10 ms duration) by NIR treatment for 180 s. The novel photonic sintering technique for STO thin films described here is a viable approach to realize room temperature *in situ* sintering process for the fabrication of flexible actuator panels.

When STO films were irradiated by a combination of NIR and deep UV during the FWL sintering process, the dielectric constant of the STO film decreased considerably (figure 4(d)). This may be because excessive irradiation energy from deep UV and NIR caused damage of the STO films.

4. Conclusion

In this study, an ultra-high speed photonic sintering method via FWL combined with NIR and deep UV light irradiations was developed in order to fabricate $SrTiO_3$ (STO) thin films for vibration touch panel applications. It was demonstrated that FWL irradiation sintered the STO films on a polymer substrate at room temperature under ambient conditions in a few milliseconds. Furthermore, it was also found that additional irradiation by deep UV and NIR combined with FWL could enhance the sintering of STO films through photocatalytic and photo-thermal reactions, respectively.

Therefore, it is expected that the newly developed photonic sintering technique of the STO films is a strong alternative for *in situ* sintering of the insulating layer in flexible actuator panels at room temperature.

Acknowledgments

This work was supported by the Basic Science Research Program through the National Research Foundation of Korea (NRF), funded by the Ministry of Education (2013M2A2A9043280 and 2015R1D1A1A09058418). Also, this research was supported by Nano-Convergence Foundation (http://www.nanotech2020.org) funded by the Ministry of Science, ICT and Future Planning (MSIP, Korea) & the

Ministry of Trade, Industry and Energy (MOTIE, Korea) [Project Number: R201502510].

References

[1] Poupyrev I and Maruyama S 2003 Tactile interfaces for small touch screens *Proc. 16th Annual ACM Symp. on User Interface Software and Technology* (ACM) pp 217–20

[2] Salisbury K, Brock D, Massie T, Swarup N and Zilles C 1995 Haptic rendering: programming touch interaction with virtual objects *Proc. 1995 Symp. on Interactive 3D Graphics* (ACM) pp 123–30

[3] Lee J C, Dietz P H, Leigh D, Yerazunis W S and Hudson S E 2004 Haptic pen: a tactile feedback stylus for touch screens *Proc. 17th Annual ACM Symp. on User Interface Software and Technology* (ACM) pp 291–4

[4] Zhu B, Wang H, Liu Y, Qi D, Liu Z, Wang H, Yu J, Sherburne M, Wang Z and Chen X 2016 Skin-inspired haptic memory arrays with an electrically reconfigurable architecture *Adv. Mater.* **28** 1559–66

[5] Larson C, Peele B, Li S, Robinson S, Totaro M, Beccai L, Mazzolai B and Shepherd R 2016 Highly stretchable electroluminescent skin for optical signaling and tactile sensing *Science* **351** 1071–4

[6] Zhu G, Yang W Q, Zhang T, Jing Q, Chen J, Zhou Y S, Bai P and Wang Z L 2014 Self-powered, ultrasensitive, flexible tactile sensors based on contact electrification *Nano Lett.* **14** 3208–13

[7] Bau O, Poupyrev I, Israr A and Harrison C 2010 Teslatouch: electrovibration for touch surfaces *Proc. 23nd Annual ACM Symp. on User Interface Software and Technology* (ACM) pp 283–92

[8] Kim S-C, Israr A and Poupyrev I 2013 Tactile rendering of 3D features on touch surfaces *Proc. 26th Annual ACM Symp. on User Interface Software and Technology* (ACM) pp 531–8

[9] Yang T, Wang W, Zhang H, Li X, Shi J, He Y, Zheng Q-S, Li Z and Zhu H 2015 Tactile sensing system based on arrays of graphene woven microfabrics: electromechanical behavior and electronic skin application *ACS Nano* **9** 10867–75

[10] Levesque V, Oram L, MacLean K, Cockburn A, Marchuk N D, Johnson D, Colgate J E and Peshkin M A 2011 Enhancing physicality in touch interaction with programmable friction *Proc. SIGCHI Conf. on Human Factors in Computing Systems* (ACM) pp 2481–90

[11] Winfield L, Glassmire J, Colgate J E and Peshkin M 2007 T-pad: tactile pattern display through variable friction reduction *2nd Joint EuroHaptics Conf. Symp. on Haptic Interfaces for Virtual Environment and Teleoperator Systems. World Haptics 2007* (Piscataway, NJ: IEEE) pp 421–6

[12] Radivojevic Z, Beecher P, Bower C, Cotton D, Haque S, Andrew P, Henson B, Wall S A, Howard I S and Ingram J N 2012 Programmable electrostatic surface for tactile perceptions *SID Symp. Digest of Technical Papers* (New York: Wiley) pp 407–10

[13] Shultz C D, Peshkin M A and Colgate J E 2015 Surface haptics via electroadhesion: expanding electrovibration with johnsen and rahbek *World Haptics Conf. (WHC), 2015* (Piscataway, NJ: IEEE) pp 57–62

[14] Mallinckrodt E, Hughes A and Sleator W Jr 1953 Perception by the skin of electrically induced vibrations *Science* **118** 277–8

[15] Guan X, Becdelievre J, Meunier B, Benali A, Saint-Girons G, Bachelet R, Regreny P, Botella C, Grenet G and Blanchard N 2016 GaAs core/$SrTiO_3$ shell nanowires grown by molecular beam epitaxy *Nano Lett.* **16** 2393–9

[16] Hu D, Ma H, Tanaka Y, Zhao L and Feng Q 2015 Ferroelectric mesocrystalline $BaTiO_3$/$SrTiO_3$ nanocomposites with enhanced dielectric and piezoelectric responses *Chem. Mater.* **27** 4983–94

[17] Yan L C, Hassan J, Hashim M, Yin W S, Khoon T F and Jeng W Y 2011 Effect of sintering temperatures on the microstructure and dielectric properties of $SrTiO_3$ *World Appl. Sci. J.* **14** 1091–94

[18] Supasai T, Dangtip S, Learngarunsri P, Boonyopakorn N, Wisitsoraat A and Hodak S K 2010 Influence of temperature annealing on optical properties of $SrTiO_3$/$BaTiO_3$ multilayered films on indium tin oxide *Appl. Surf. Sci.* **256** 4462–7

[19] Hwang H-J and Kim H-S 2015 Ultra-high speed fabrication of TiO_2 photoanode by flash light for dye-sensitized solar cell *J. Nanosci. Nanotechnol.* **15** 5028–34

[20] Hwang H-J, Joo S-J and Kim H-S 2015 Copper nanoparticle/multiwalled carbon nanotube composite films with high electrical conductivity and fatigue resistance fabricated via flash light sintering *ACS Appl. Mater. Interfaces* **7** 25413–23

[21] Tahan D M, Safari A and Klein L C 1996 Preparation and characterization of Ba_xSr_{1-x}, TiO_3 thin films by a sol–gel technique *J. Am. Ceram. Soc.* **79** 1593–8

[22] Wu D, Li A, Liu Z, Ling H, Ge C Z, Liu X, Wang H, Wang M, Lü P and Ming N 1998 Fabrication and electrical properties of sol–gel derived (BaSr) TiO_3 thin films with metallic $LaNiO_3$ electrode *Thin Solid Films* **336** 172–5

[23] Wu D, Li A, Ling H, Yin X, Ge C, Wang M and Ming N 2000 Preparation of ($Ba_{0.5}Sr_{0.5}$) TiO_3 thin films by sol–gel method with rapid thermal annealing *Appl. Surf. Sci.* **165** 309–14

[24] Liu J, Zhang L, Li N, Tian Q, Zhou J and Sun Y 2015 Synthesis of MoS_2/$SrTiO_3$ composite materials for enhanced photocatalytic activity under UV irradiation *J. Mater. Chem.* A **3** 706–12

[25] Bergmann C P and de Andrade M J 2011 *Nanostructured Materials for Engineering Applications* (Berlin: Springer) (doi:10.1007/978-3-642-19131-2)

[26] Hwang H-J, Oh K-H and Kim H-S 2016 All-photonic drying and sintering process via flash white light combined with deep-UV and near-infrared irradiation for highly conductive copper nano-ink *Sci. Rep.* **6** 19696

[27] German R M 1996 *Sintering Theory and Practice* (Hoboken, NJ: Wiley-VCH) p 568